Immunohistochemical and Biogenetic Features of Diffuse-Type Tenosynovial Giant Cell Tumors: The Potential Roles of Cyclin A, P53, and Deletion of 15q in Sarcomatous Transformation

Hsuan-Ying Huang,[1] Robert B. West,[4] Ching-Cherng Tzeng,[5] Matt van de Rijn,[4] Jun-Wen Wang,[2] Shih-Cheng Chou,[3] Wen-Wei Huang,[6] Hock-Liew Eng,[1] Ching-Nan Lin,[5] Shih-Chen Yu,[1] Jing-Mei Wu,[1] Chiu-Chin Lu,[1] and Chien-Feng Li[5]

Abstract

Purpose: Diffuse-type tenosynovial giant cell tumor (D-TSGCT) is an aggressive proliferation of synovial-like mononuclear cells with inflammatory infiltrates. Despite the *COL6A3-CSF1* gene fusion discovered in benign lesions, molecular aberrations of malignant D-TSGCTs remain unidentified.

Experimental Design: We used fluorescent *in situ* hybridization and *in situ* hybridization to evaluate *CSF1* translocation and mRNA expression in six malignant D-TSGCTs, which were further immunohistochemically compared with 24 benign cases for cell cycle regulators involving G_1 phase and G_1-S transition. Comparative genomic hybridization, real-time reverse transcription-PCR, and a combination of laser microdissection and sequencing were adopted to assess chromosomal imbalances, cyclin A expression, and *TP53* gene, respectively.

Results: Five of six malignant D-TSGCTs displayed *CSF1* mRNA expression by *in situ* hybridization, despite only one having *CSF1* translocation. Cyclin A ($P = 0.008$) and P53 ($P < 0.001$) could distinguish malignant from benign lesions without overlaps in labeling indices. Cyclin A transcripts were more abundant in malignant D-TSGCTs ($P < 0.001$). All malignant cases revealed a wild-type *TP53* gene, which was validated by an antibody specifically against wild-type P53 protein. Chromosomal imbalances were only detected in malignant D-TSGCTs, with DNA losses predominating over gains. Notably, -15q was recurrently identified in five malignant D-TSGCTs, four of which showed a minimal overlapping deletion at 15q22-24.

Conclusions: Deregulated *CFS1* overexpression is frequent in malignant D-TSGCTs. The sarcomatous transformation involves aberrations of cyclin A, P53, and chromosome arm 15q. *Cyclin A* mRNA is up-regulated in malignant D-TSGCTs. Non–random losses at 15q22-24 suggest candidate tumor suppressor gene(s) in this region. However, P53 overexpression is likely caused by alternative mechanisms rather than mutations in hotspot exons.

Authors' Affiliations: Departments of [1]Pathology and [2]Orthopedic Surgery, Chang Gung Memorial Hospital-Kaohsiung Medical Center, Chang Gung University College of Medicine, [3]Department of Pathology and Laboratory Medicine, Veterans General Hospital-Kaohsiung, Kaohsiung, Taiwan, [4]Department of Pathology, Stanford University Medical Center, Stanford, California, [5]Department of Pathology, Chi-Mei Foundation Medical Center, Tainan, Taiwan, and [6]Department of Family Medicine, Buddhist Dalin Tzu Chi General Hospital, Chiayi, Taiwan

Received 2/19/08; revised 5/28/08; accepted 6/3/08.

Grant support: National Science Council, Taiwan (NSC 95-2320-B-182A-007-MY2), Chang Gung Memorial Hospital (CMRPG83019II, CMRPG83038), and Chi-Mei Medical Center (CMFHR 9568).

The costs of publication of this article were defrayed in part by the payment of page charges. This article must therefore be hereby marked *advertisement* in accordance with 18 U.S.C. Section 1734 solely to indicate this fact.

Note: Supplementary data for this article are available at Clinical Cancer Research Online (http://clincancerres.aacrjournals.org/).

This work has been presented in part at the 96th annual meeting of the United States and Canadian Academy of Pathology, San Diego, CA. March 24-30, 2007.

Requests for reprints: Chien-Feng Li, Department of Pathology, Chi-Mei Foundation Medical Center, Tainan, Taiwan. Phone: 886-6281-2811, ext. 53680; Fax: 886-6251-1235; E-mail: cfli.hyhuang@gmail.com.

doi:10.1158/1078-0432.CCR-08-0252

Tenosynovial giant cell tumors (TSGCT) are unique mesenchymal lesions that arise from the synovial lining of articular spaces, bursal sacs, and tendon sheaths (1, 2). The neoplastic property of TSGCTs has been supported by the identification of DNA aneuploidy and clonal karyotypic aberrations in these tumors, such as trisomies 7 and 5 and/or translocations involving chromosomal regions 1p11-13, 2q35-37, or 16q22-24 (2–6). Given the difference in clinical behavior, TSGCTs are further divided by growth patterns into localized and diffuse types and by the predominant location of occurrence into extra-articular and intra-articular forms (1–4). Histologically, diffuse-type TSGCT (D-TSGCT), i.e., pigmented villonodular synovitis if located intra-articularly, is an infiltrative proliferation of synovial-like mononuclear cells accompanied by heterogeneous inflammatory infiltrates among varying degrees of collagenous stroma (1, 2, 7). It frequently develops multiple local recurrences that are sometimes difficult to control by surgical excision and can severely compromise joint function (1, 2).

In the absence of sarcomatous transformation, it is extremely rare for D-TSGCT to develop distant metastasis (1, 2, 7, 8). However, malignant D-TSGCT is characterized by an apparently

Translational Relevance

Similar to benign lesions, deregulated *CFS1* mRNA overexpression, as detected by *in situ* hybridization, is also frequent in malignant D-TSGCT. This suggests a central pathogenetic role for *CFS1* deregulation in the early stage of TSGCTs. However, the separation of benign from malignant D-TSGCTs can be challenging on a purely morphologic basis. This study showed that alterations in cyclin A, P53, and chromosome arm 15q are present in the majority of malignant D-TSGCTs but not in benign lesions, which represent critical events in sarcomatous transformation. Combined evaluation of *CSF1* expression status and aberrations of cyclin A, P53, and chromosome arm 15q may aid in the differential diagnosis and prediction of sarcomatous transformation in D-TSGCTs.

higher metastatic propensity with considerable tumor-related mortality, based on the clinical outcomes of 33 such cases reported to date (5, 7, 9, 10). In this context, malignant D-TSGCT merits recognition as an exceptionally rare but distinct tumor entity. Histologically, it contains a frank sarcoma associated with a preceding or concurrent typical benign D-TSGCT (7, 8), as initially set forth by Enzinger and Weiss (8). Intriguingly, some authors previously implied that D-TSGCTs should also be considered to be "malignant" due to its aggressive nature, although the morphologic appearance may remain unaltered during the course of the disease (8). Making the issues of nomenclature and diagnosis more complicated, others accepted all giant cell–containing sarcomas that originated within or adjacent to tenosynovial structure as malignant D-TSGCTs. The latter lumping approach might result in erroneous inclusion of a variety of mimicking lesions in the past, such as clear cell sarcoma or malignant fibrous histiocytoma of giant cell type, etc. (8). These diagnostic difficulties reflect considerable morphologic variation in the associated sarcomatous component of malignant D-TSGCTs, thereby posing a great challenge in prognostication and treatment decision.

Benign TSGCTs have recently been characterized by the discovery of *COL6A3-CSF1* gene fusion derived from a recurrent chromosomal translocation, t(1; 2)(p13;q37) (ref. 11). This chimeric fusion in a minority of tumor cells results in the activation of CSF1 expression, which creates a "landscape" effect to increase neoplastic cells through an autocrine loop with CSF1R (11). In addition, CSF1 may recruit the more abundant, CSF1R-expressing inflammatory cells (11). To our knowledge, pathogenetic mechanisms of malignant D-TSGCTs remain, thus far, unknown. Therefore, it is highly desirable to identify critical molecular alterations implicated in the malignant transformation of benign lesions. In translocation-associated tumors, secondary deregulation of cell cycle regulators is thought to promote tumor progression, thereby conferring an adverse prognostic effect (12, 13). According to previous studies, chromosomal abnormalities in this type of neoplasm tend to be relatively few but apparently contribute to clinical aggressiveness (14). In this regard, comparative genomic hybridization (CGH) can serve as genomewide screening in these tumors to search for crucial secondary genomic gains or losses implicated in tumor progression (15, 16), although it is unable to detect the initiating reciprocal translocations per se (16).

Accordingly, the aims of this study on the pathogenesis of malignant D-TSGCTs were 2-fold: first, by fluorescent *in situ* hybridization (FISH) and *in situ* hybridization (ISH), we investigated whether translocation and mRNA overexpression of the *CSF1* gene also occur in malignant D-TSGCTs, as reported previously in benign TSGCTs (11, 17). Second, we assessed whether malignant phenotypes of D-TSGCTs are attributed to the deregulated early G_1 and G_1-S transition checkpoints and/or non–random chromosomal aberrations, like other tumors with a specific chimeric oncogene (e.g., Ewing sarcoma; ref. 13). For the second issue, a panel of cell cycle regulators was evaluated by immunohistochemistry for both

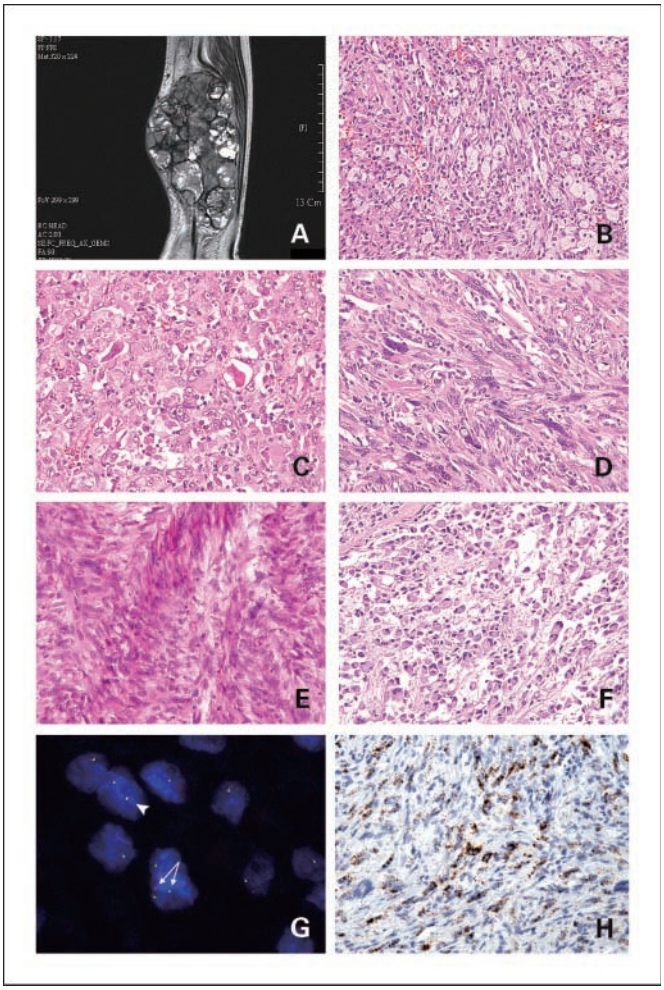

Fig. 1. Radiological, histologic, and FISH/ISH findings in malignant D-TSGCTs. *A,* coronal T1-weighted magnetic resonance image of a representative case showed an extensively infiltrative mass of the right leg with heterogeneous hyperintensities. *B,* the associated histologically benign areas comprised rounded, mononuclear tumor cells admixed with heterogeneous infiltrates of lipid-laden histiocytes and lymphocytes. In the sarcomatous areas of malignant D-TSGCT, the histologic patterns included the giant cell tumor–like (*C*), malignant fibrous histiocytoma–like (*D*), fibrosarcomatous (*E*), and myxosarcomatous (*F*) architectures. FISH assay using *CSF* (1p13) break-apart probe (*G*) showed a translocation (*arrows,* split red and green signals) and another intact signal (*arrowhead,* fused red and green signals) in a representative tumor nucleus of malignant D-TSGCT (case 3). *H,* chromogenic RNA ISH revealed strong expression of CSF1 expression in atypical spindle sarcoma cells.

malignant and benign D-TSGCTs to better characterize immunophenotypic and potential biogenetic alterations related to sarcomatous transformation. We found that overexpression of cyclin A and P53 proteins could robustly distinguish between these two groups without overlap in labeling indices. Accordingly, we did additional real-time reverse transcription-PCR assays for *cyclin A* to compare the difference in mRNA expression levels between malignant and benign cases. In addition, the genomic status in hotspot exons of *TP53* gene were determined for the sarcomatous component of malignant D-TSGCTs by coupling laser capture microdissection (LCM) with bidirectional sequencing as well as immunostaining with a wild-type P53-specific antibody. Lastly, chromosomal alterations were analyzed by CGH for all malignant D-TSGCTs and selected benign control cases to compare the differences in the pattern of imbalances and to search critical regions related to sarcomatous transformation.

Materials and Methods

Inclusion criteria, case selection, and tissue specimens. The criteria for case selection have been recently described in a separate article addressing the clinicopathologic features and outcomes of malignant D-TSGCTs (7). In brief, we diagnosed a malignant D-TSGCT when it arose from or near the large joint (Fig. 1A) and displayed frankly sarcomatous histology at the same site of either a concurrent (*de novo*) or previous (metachronous) benign D-TSGCT (7, 8). After histologic and radiological reviews, paraffin tissue blocks of six surgically treated malignant D-TSGCTs, including four *de novo* and two metachronous cases (cases 1-4, 6, and 7 in Li et al.'s article; ref. 7), were available for immunohistochemical and molecular studies.

FISH and ISH for translocation and expression of CSF1. To evaluate the status of *CSF1* translocation, FISH was done in six malignant D-TSGCTs. Chromogenic RNA ISH was also used in these cases to assess *CSF1* mRNA expression. The protocols for FISH and ISH have been previously described (11, 17). The results of *CSF1* break-apart FISH were determined by analyzing a minimum of 25 lesional cells, based on nuclear size and location within the tumor. Lesional cells were classified according to the distance between the break-apart probe pairs or the loss of one of the break-apart probes. A locus alteration was called if a consistent change was seen in at least 50% of the lesional cells.

Immunohistochemistry. Immunohistochemical studies were done on 3-μm-thick sections from paraffin blocks available in 6 malignant and 24 randomly selected benign D-TSGCTs, using the following antibodies and dilution folds: cyclin A (6E6, 1:50; Novocastra), cyclin E (13A3, 1:40; Novocastra), cyclin D1 (SP4, 1:100; LabVision), P53 (DO-7, 1:1,000; Serotec), P16 (6H12, 1:20; Novocastra), and P27 (1B4, 1:20; Novocastra). The DO-7 P53 antibody was previously known to react to both wild-type and mutant P53 proteins. Another monoclonal antibody recognizing only the wild-type P53 protein (Ab-5, 1:20; Oncogene) was used to distinguish the status of overexpressed P53 for six malignant D-TSGCTs (18). For antigen retrieval, slides were pressure-cooked in 10 mmol/L of citrate buffer at pH 6 for 7 min and washed using TBS buffer with 0.1% Tween 80. Endogenous peroxidase activity was quenched by 3% H_2O_2 treatment. Except for incubation overnight with P53/Ab-5, the slides were incubated for 1 h at room temperature with all other primary antibodies and detected by using the ChemMate DAKO EnVision kit (DAKO, K5001) according to the manufacturer's instruction. For the aforementioned antibodies, the percentages of cells with nuclear staining were counted for a minimum of 1,000 mononuclear and bizarre pleomorphic tumor cells in the most active areas and expressed as labeling indices.

Real-time quantitative reverse transcription-PCR to detect cyclin A mRNA expression. For real-time reverse transcription-PCR assays, special attention was paid to the tissue sectioning step by changing the microtome blade between each block to avoid potential contamination. To extract total RNA from paraffin-embedded tissues for measuring *cyclin A* mRNA expression, eight 10-μm whole tissue sections were cut for each specimen from six malignant and eight benign D-TSGCTs. In parallel, the synovial tissues from five cases with degenerative tenosynovial or joint disorders were cut and extracted to serve as calibrator controls. Total RNA was extracted using RecoverAll total nucleic acid isolation kit (Ambion) following the manufacturer's protocols. Briefly, tissue sections were dewaxed in xylene, washed twice with ethanol, air-dried, incubated with protease at 50°C for 3 h, and extracted with the mixture of isolation additive and ethanol. The suspension was purified using a filter cartridge, digested with DNAse for 30 min to remove residual DNA, and then washed thrice with provided buffers to acquire 32 μL of RNA eluant. By using ImProm-II reverse transcription system (Promega), RNA samples were reverse-transcribed in a final volume of 40 μL under the following conditions: 0.5 mmol/L deoxynucleotide triphosphates, 25 units of RNase inhibitor, 16 μL of RNA eluant, and 4 μL of random primers. The reactions were done at 42°C for 60 min, followed by inactivation of the enzyme at 70°C for 15 min. Real-time reverse transcription-PCR assay for *cyclin A* mRNA quantification was done using the LightCycler instrument 2.0 (Roche Molecular Diagnostics). Intron-spanning primers and prevalidated LON probes for transcripts of *cyclin A* (*CCNA2*) and housekeeping *POLR2A* gene (RNA polymerase II, polypeptide A a.k.a. RPII) were designed online with the ProbeFinder software[7] and ordered from Universal ProbeLibrary (Roche Molecular Diagnostics). *POLR2A* was selected as the endogenous reference because it proved to be the gene with the most constant expression in a broad range of tissues (19). The amplicon sizes of *cyclin A* and *POLR2A* cDNAs, and the corresponding sequences of specific PCR primer pairs and probes were listed in Supplementary Table S1. Amplification was conducted with LightCycler TaqMan MasterMix (Roche Applied Science) using 10 μL of cDNAs, 100 nmol/L of the probes, and 200 nmol/L of the primers in a final 20 μL of reaction mixture. After 2 min incubation at 40°C to allow for uracil *N*-glycosylase cleavage, Taq DNA polymerase was activated by incubation for 10 min at 95°C. Each reaction of the 45 PCR cycles consisted of 10 s of denaturation at 95°C and hybridization of the probe and primers for 30 s at 60°C and was done in duplicate. Fluorescence curves were plotted and analyzed by LightCycler software version 4.0 to determine the values of crossing points (Cp), defined as the maximum of the second derivative of the fluorescence curves. Relative expression level of *cyclin A* mRNA was calculated using the comparative C_T (Cp) method. The amount of *cyclin A*, after normalization to *POLR2A*, was then given by $2^{-\Delta\Delta Cp}$, where $\Delta\Delta Cp = \Delta Cp$ (sample) - ΔCp (calibrator: the mean of five degenerative synovial tissue specimens), and ΔCp represented the Cp of *cyclin A* subtracted from the Cp of *POLR2A* (20). Only samples with consistent amplification of *POLR2A*, i.e., Cp < 32, were included in the final analyses, whereas those with higher Cp values for *POLR2A* were considered uninterpretable because of poor RNA quality (21).

Mutation analysis of* TP53 *gene by LCM coupled with PCR/bidirectional sequencing. To circumvent the contaminating artifacts of numerous surrounding inflammatory and stromal cells, we adopted LCM technology to isolate pure sarcoma cells for mutation analysis of *TP53* gene. One representative paraffin block in each case of six malignant D-TSGCTs was recut, stained with HistoGene LCM Staining Kit (Arcturus Engineering, Inc.), and placed onto a PEN-membrane slide to isolate cells of interest by using an automated LCM system (Veritas, Arcturus Engineering, Inc.). Approximately 2,500 cells were collected on the Capsure Macro cap, extracted by Picopure DNA isolation kit (Arcturus Bioscience) at 65°C overnight with 50 μL of provided buffer, and then desalted by microspin column (Amersham Biosciences). By using primers from published sequences at National

[7] https://www.roche-applied-science.com/sis/rtpcr/upl/adc.jsp

Table 1. Clinicopathologic features of six malignant D-TSGCTs and results of translocation and expression of *CSF1*

Cases	Age (y)/sex*	Location	Size (cm) †	Type	Nature	Histology †	Mitotic count †
Case 1	45/M	Ankle	8	I	Metachronous (7 mo) ‡	FS-like	6/10 HPFs
Case 2	78/F	Knee	8	E	*De novo*	MFH-like	18/10 HPFs
Case 3	39/F	Forearm	12	E	Metachronous (31 y) ‡	MS-like	2/10 HPFs
Case 4	52/M	Suprapopliteal	10	E	*De novo*	MFH-like	3/10 HPFs
Case 5	67/F	Lower leg	17	E	*De novo*	GCT-like	56/10 HPFs
Case 6	46/F	Thigh	5	E	*De novo*	MFH-like	34/10 HPFs

Abbreviations: AWD, alive with disease; DOD, dead of disease; E, extra-articular; F, female; FS, fibrosarcoma; GCT, giant cell tumor; HPF, high-power field; I, intra-articular; M, male; MFH, malignant fibrous histiocytoma; MS, myxosarcoma; NED, no evidence of disease; R/T, radiation therapy.

*Age at initial diagnosis of either the primary malignant TSGCT or the preceding benign tumor of metachronous malignant D-TSGCT.

† Specified for malignant tumors, either *de novo* or metachronous.

‡ Time interval in diagnoses between primary benign and metachronous malignant TSGCTs.

Center for Biotechnology Information web site, the hotspots of somatic *TP53* mutation, i.e., exons 5 to 9, were amplified by PCR as follows: an amount of 5 μL of DNA was subjected to 40 cycles of PCR in a final reaction volume of 50 μL, which contained 5 μmol/L of each oligonucleotide primer, 2.5 units of Platinum Taq DNA polymerase (Invitrogen), 4 μL of deoxynucleotide triphosphate mixture at 10 mmol/L, 33.5 μL of double-distilled water, 2 mmol/L of $MgCl_2$, and 5 μL of 10× PCR buffer. Except for exon 5, 3 μL of 50-fold diluted first PCR products was used as the DNA template of nested PCR for exons 6 to 9. PCR conditions were 94°C for 25 s, annealing temperature of each primer set (see Supplementary Table S1) for 45 s, and 72°C for 45 s. Nested PCR products were electrophoresed on 2% agarose gel, and the amplified DNA fragments were purified and then bidirectionally sequenced using an ABI prism 3730 Sequencer (Applied Biosystems).

CGH. The procedure of CGH was based on Kallioniemi's method with minor modifications (15, 16). For each specimen with available paraffin blocks, four 30-μm tissue sections were cut from the same six malignant and eight benign D-TSGCTs subjected to real-time reverse transcription-PCR assay. Tissue sections were dewaxed in xylene, washed with absolute ethanol and allowed to air-dry, and then digested overnight at 55°C with 0.5 mg/mL of proteinase K solution (Sigma) containing 10 mmol/L of Tris (pH 7.8), 5 mmol/L of EDTA, and 0.5% SDS. Subsequently, DNA suspension was purified by phenol/chloroform and resuspended in 1× TE buffer. Metaphase slides were made from peripheral blood lymphocytes of normal males using standard protocols with the inclusion of methotrexate and thymidine for synchronization. Only slide batches showing strong uniform hybridization fluorescence signals were chosen for further experimental use.

Reference DNA was prepared from peripheral blood lymphocytes of women with a normal karyotype using a commercial kit (Puregene). By using nick translation, tumor DNA and reference DNA were directly labeled using fluorescein-12-dUTP or Texas red-5-dUTP (NEN Life Science), respectively. Four hundred nanograms of labeled tumor DNA, 400 ng of labeled reference DNA, and 10 μg of unlabeled *Cot*1 DNA (Life Technologies) were coprecipitated and resuspended in 10 μL of a hybridization solution (70% formamide, 2× SSC, and 10% dextran sulfate). The probe mixture was denatured at 70°C for 5 min and hybridized to metaphase slides at 37°C in a humid chamber for 2 days. Prior to hybridization, the slides were denatured by incubation in 70% formamide, 2× SSC at 74°C for 3 min and dehydrated in an ascending graded series of alcohol. Slides were rinsed in 50% formamide twice, in 2× SSC solution at 45°C and room temperature for 10 min each, and thrice in PN buffer at room temperature for 10 min. After air-drying, the slides were counterstained with 4′,6-diamidino-2-phenylindole in an antifading solution (200 ng/mL in 2× SS, H-1000; Vector Laboratories). Images from representative metaphase spreads were acquired by an Olympus fluorescence microscope (BX51) adapted to a Sensys CCD camera (Kodak KAF 1400 chip; Photometrics) and digitalized using a Cytovision imaging system (Applied Imaging). Karyotypes from 12 to 15 metaphases were combined to generate a mean CGH ratio profile for each test sample. Chromosomally imbalanced alterations were determined based on the calculation of standard reference intervals using CytoVision High-Resolution CGH software, by which we stringently defined DNA losses or gains as significant whenever the tumor profile and the standard reference interval profile at 99.5% confidence did not overlap (22). However, short chromosomal segments with a test-to-reference fluorescence ratio of >1.5 were construed as showing high-level amplification.

Statistical analyses. The differences in the results of immunohistochemical staining and real-time reverse transcription-PCR assay between benign and malignant D-TSGCTs were examined by Student's *t* test. $P < 0.05$ was considered to be statistically significant.

Results

Clinicopathologic findings and follow-up. The salient clinicopathologic features and follow-up information of six malignant D-TSGCTs are summarized in Table 1. The age at diagnosis of malignant D-TSGCTs, including one intra-articular and five extra-articular lesions, ranged from 46 to 78 years (mean, 59.7) in two male and four female patients. These six cases were 5 to 17 cm (mean, 10 cm) in size and located either within or near large joints of the extremities. The detailed radiological, histomorphologic, and follow-up data of these six tumors were elaborated elsewhere (7). In the four *de novo* malignant D-TSGCTs, typical benign areas (Fig. 1B) were

Table 1. Clinicopathologic features of six malignant D-TSGCTs and results of translocation and expression of *CSF1* (Cont'd)

Necrosis †	Treatment †	Recurrence or metastasis (duration) †	Follow-up/status †	*CSF1* rearrangement (FISH)	*CSF1* expression (ISH)
Present	Tumor excision	Spinal metastases (9 mo)	10 mo/DOD	Absent	Positive
Present	Tumor excision	Local recurrences, twice (12, 27 mo)	36 mo/NED	Absent	Positive
Present	Amputation and R/T	Axillary nodal metastases (11 mo); pulmonary metastasis (22 mo)	17 mo/AWD	Present	Positive
Present	Wide tumor excision	None	12 mo/NED	Absent	Positive
Present	Tumor excision	None	8 mo/NED	Absent	Positive
Present	Wide tumor excision and R/T	Inguinal nodal metastases (9 mo)	10 mo/NED	Absent	Negative

concurrent with frank sarcomas of various morphologic types, including the giant cell tumor–like histology in one case (Fig. 1C) and the malignant fibrous histiocytoma–like (Fig. 1D) pattern in three cases. Two malignant D-TSGCTs were metachronous in tumor evolution, and fibrosarcomatous (Fig. 1E) and multinodular myxosarcomatous (Fig. 1F) areas appeared only in the first (case no. 1) and fourth (case no. 3) recurrences. After the diagnosis of malignancy, one patient subsequently developed local recurrences twice and was treated with surgical re-excision. Metastatic disease was noted in three patients, one with lumbar vertebrae involvement, another with both multiple axillary lymph node and lung metastases, and a third with inguinal lymph node involvement. The patient with distant metastasis to the spine eventually died of disease.

Findings of FISH and ISH. Distinct *CSF1* RNA expression was present in a subset of pleomorphic and/or spindle sarcoma cells (Fig. 1G; Table 1) in five of six malignant D-TSGCTs tested for ISH assay. One case (case no.3) also harbored rearranged *CSF1* gene (Fig. 1G; Table 1) as detected by the locus-specific, split-apart FISH probe. In addition, ISH also showed expression of *CSF1* receptor mRNA in the majority of both sarcomatous and heterogeneous inflammatory cells (data not shown).

Immunohistochemical expression of cell cycle regulators. The immunohistochemical findings of cell cycle regulators are shown in Fig. 2 and tabulated in Supplementary Table S2. When compared with 24 benign controls, cyclin A (Fig. 2A-C, $P = 0.002$), P53 (Fig. 2D-F, $P = 0.029$), and cyclin E (Fig. 2G-I, $P = 0.043$) showed significantly higher expression in the six malignant D-TSGCTs, although only cyclin A and P53 could robustly distinguish malignant from benign cases without overlaps in the labeling indices. In contrast, there was no significant difference in the expression of cyclin D1 (Fig. 2J-L), P27 (Fig. 2M-O), and P16 (Fig. 2P-R) between the two groups. Based on these findings, we further specifically explored the potential molecular abnormalities underlying overexpression of both cyclin A and P53.

Molecular assays. Real-time reverse transcription-PCR measurement of *cyclin A* mRNA could be successfully determined with sufficient RNA yields in five of six malignant D-TSGCTs and in seven of eight benign lesions tested. As shown in Fig. 3, the normalized relative expression copies of cyclin A mRNA were 3.25-fold more abundant ($P < 0.001$) in malignant D-TSGCTs (mean, 11.1649; range, 6.6576-14.3452) compared with those detected in the benign counterparts (mean, 3.4409; range, 0.9138-7.2854). This result suggested that up-regulated transcriptional activity could translate into overexpression of cyclin A protein, whereas the possibility of *CCNA2* gene amplification as a more upstream oncogenic alteration could not be excluded.

Using LCM to isolate pure sarcoma cells (Fig. 4A-C), we found that there was no intragenic mutation in exons 5 to 9 of the *TP53* gene in any of the six malignant D-TSGCTs sequenced bidirectionally. Furthermore, distinct overexpression of wild-type P53 protein was also substantiated in these malignant D-TSGCTs by immunohistochemistry with a specific Ab-5 antibody that does not cross-react to mutant P53 (Fig. 4A-D). These findings indicated that alternative mechanisms, instead of hotspot mutations, might operate in malignant D-TSGCTs to result in accumulation of wild-type P53 protein.

Among cases subjected to CGH, chromosomal imbalanced alterations were identified in six malignant D-TSGCTs but not in any of the eight benign lesions. Chromosomal losses were predominant over gains in these six malignant cases as illustrated in Fig. 5. The mean value of changes per tumor was 10.67 (losses, 9.83; gains, 0.83), whereas no whole chromosomal aberration was discerned. DNA gains were detected in three cases and involved only three chromosomal regions. Of note, high-level amplifications of 3p12 were seen in two cases. As for DNA losses, the frequently affected chromosome arms were 15q in five cases and 2p, 9q, 16p, and 22q in three cases each. In all five malignant cases showing aberrations of 15q, 15q22-24 was found to be the minimal overlapping region of chromosomal deletion in four cases.

Discussion

Great histomorphologic variation can be present in the sarcomatous areas of malignant D-TSGCT, which is a distinct sarcoma entity with considerable mortality and metastatic potential, including a preference of spreading to regional lymph nodes (7). However, there have been no studies thus far reporting specific molecular aberrations to portend malignant transformation of benign D-TSGCTs. Given that the separation of benign from malignant D-TSGCTs can be challenging on a purely morphologic basis (1, 3, 5, 7–9), our goals were to identify molecular determinants whose genetic

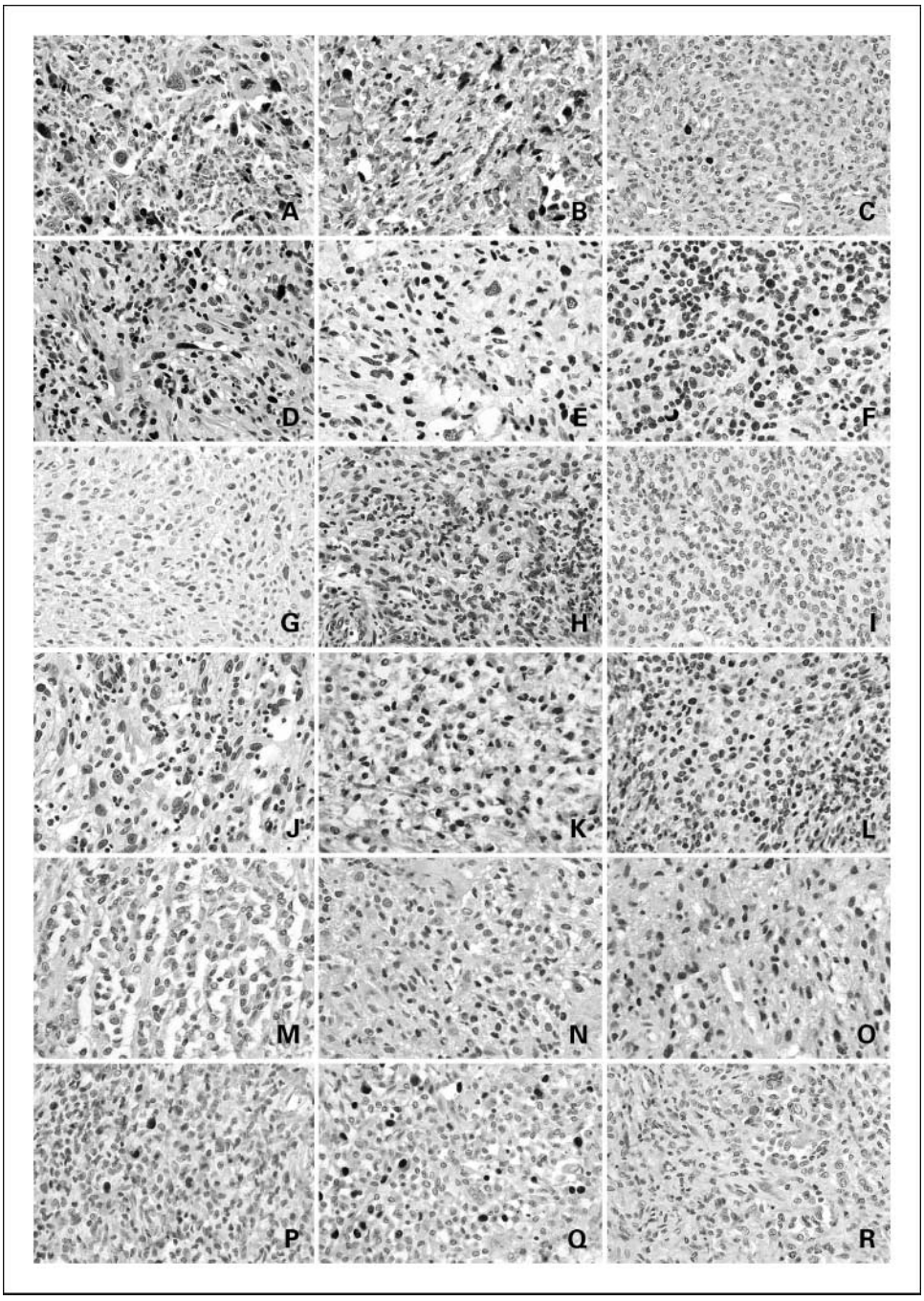

Fig. 2. Immunohistochemical expression of cyclin A (*A-C*), P53 (*D-F*), cyclin E (*G-I*), cyclin D1 (*J-L*), P27 (*M-O*), and P16 (*P-R*) in two representative malignant (case nos. 2 and 3, *left* and *middle columns*) and one benign but mitotically active TSGCTs (*right column*). Malignant TSGCTs showed higher labeling indices of cyclin A (*A* and *B*), P53 (*D* and *E*), and cyclin E (*G* and *H*) as compared with the benign case (*C,* cyclin A; *F,* P53; *I,* cyclin E). The expressions of cyclin D, P27, and P16 were not significantly different between malignant and benign cases.

changes and/or expression may aid in differential diagnosis, prognostication, and perhaps, treatment decision. The present study shows that similar to its benign counterpart, the involvement of *CSF1* is frequently detected in malignant D-TSGCTs. The alterations in the expression of P53 and cyclin A as well as the deletion at 15q22-24 are uniquely implicated in the sarcomatous transformation of D-TSGCTs.

The finding that five of our six malignant D-TSGCTs exhibited *CSF1* mRNA expression was generally in keeping with the frequency seen in benign TSGCTs from prior reports (11, 17). This suggests a pathogenetic role of deregulated *CSF1* overexpression in the early stage of TSGCTs that may progress to malignant tumors if additional molecular aberrations were superimposed on the sustained *CSF1-CSF1R* tyrosine kinase pathway activity. The high levels of *CSF1* expression are known to link with the chimeric fusion between *COL6A3* and *CSF1* genes (11), although this translocation does not seem to be universally present in each case (11, 17). Nevertheless, we are not yet clear about whether the lower frequency (1/6) of *CSF1* translocation in malignant TSGCTs was ascribed to the small sample size or whether it might reflect a more frequent occurrence of unrecognized alternative mechanisms leading to *CSF1* overexpression (23).

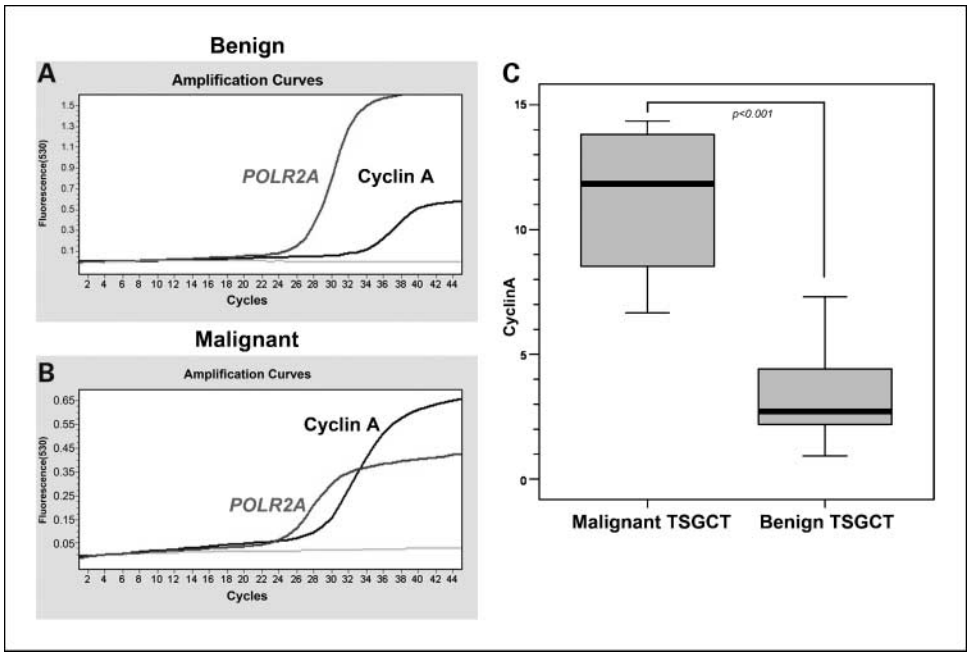

Fig. 3. Representative curves of real-time PCR quantification for cyclin A mRNA expression in benign (*A*) and malignant (*B*) TSGCTs. The normalized relative abundance of cyclin A mRNA (*C*) were significantly higher ($P < 0.001$) in malignant TSGCTs than in the benign counterparts.

Deregulated cell growth is the most fundamental attribute of tumor development and progression. As a cyclin species with multiple roles in the cell cycle, the expression of cyclin A is not only involved in S phase progression, G_2-M phase transition, and initiation of mitosis but is also closely linked to the cell proliferation rate (24). Cyclin A overexpression has been proven to correlate with tumor progression and/or adverse outcomes in a variety of cancers, including soft tissue sarcomas (24, 25). In this study, we have shown the overexpression of cyclin A protein in malignant D-TSGCTs with an average labeling index that was significantly higher and showed no overlap in the distribution range compared with benign lesions. Moreover, the abundance of *cyclin A* mRNA was also significantly increased in malignant D-TSGCTs, suggesting that cyclin A expression is primarily regulated at the transcriptional and/or genomic level, rather than through a posttranscriptional mechanism mediating protein degradation. Specifically for translocation-associated sarcoma, increased expression of cyclin A in synovial sarcomas was found to be associated with the *SYT-SSX1* fusion type, a variant subtype conferring higher proliferative activity (26). It seems tempting to speculate that the *COL6A3-CSF1* gene fusion, or some yet unknown but functionally similar genetic variation, could differentially affect the cell cycle machinery, thereby modulating the transcription of *cyclin A* in D-TSGCTs.

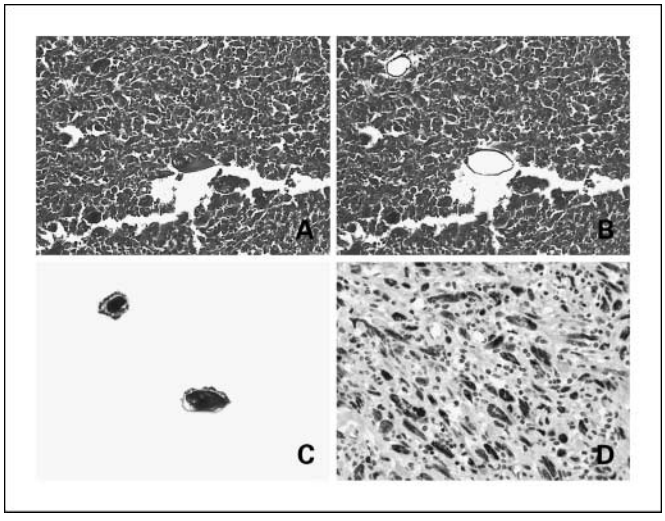

Fig. 4. LCM was applied to isolate pure sarcoma cells for mutation analysis of exons 5 to 9 of *TP53* gene. The representative images of a malignant D-TSCGT (case no. 5) before (*A*) and after (*B*) capture were shown, together with bizarre sarcoma cells of interest in the collection cap (*C*). All five malignant cases tested showed wild-type *TP53* gene by sequencing, which was also immunohistochemically validated by distinct overexpression of wild-type P53 protein using the specific Ab-5 antibody (*D*).

The expression of P53 protein is mainly regulated in the posttranscriptional stage and maintained at a low level with a short half-life in unperturbed cells (27, 28). In response to various cellular stresses, such as DNA damage and mitogenic signaling, a prompt increase in the intracellular level of functional P53 protein is required for the prevention of genomic instability and oncogenic transformation (27, 28). In this series, the apparent P53 protein overexpression detected by DO-7 antibody suggested that stabilization of either wild-type or mutant protein preferentially occur in malignant D-TSGCTs but not in benign lesions. Nevertheless, we could not detect intragenic mutations in hotspot exons 5 to 9 of the *TP53* gene in pure sarcoma cells of any malignant D-TSGCT. Recently, Das et al. showed that soft tissue sarcomas might have a higher prevalence of *TP53* exon 4 mutations than previously thought (29). Accordingly, the possibility of mutations outside the classical core-binding domain of *TP53* could not be completely excluded in malignant D-TSGCTs (27, 28, 30). However, the strong staining with the wild-type–specific Ab-5 antibody in pleomorphic sarcoma cells corroborates our sequencing results, indicating that the P53 protein in malignant D-TSGCTs is most likely wild-type and possibly accumulates via alternative mechanisms leading to protein stabilization (18). Indeed, there are many human cancers without mutations in

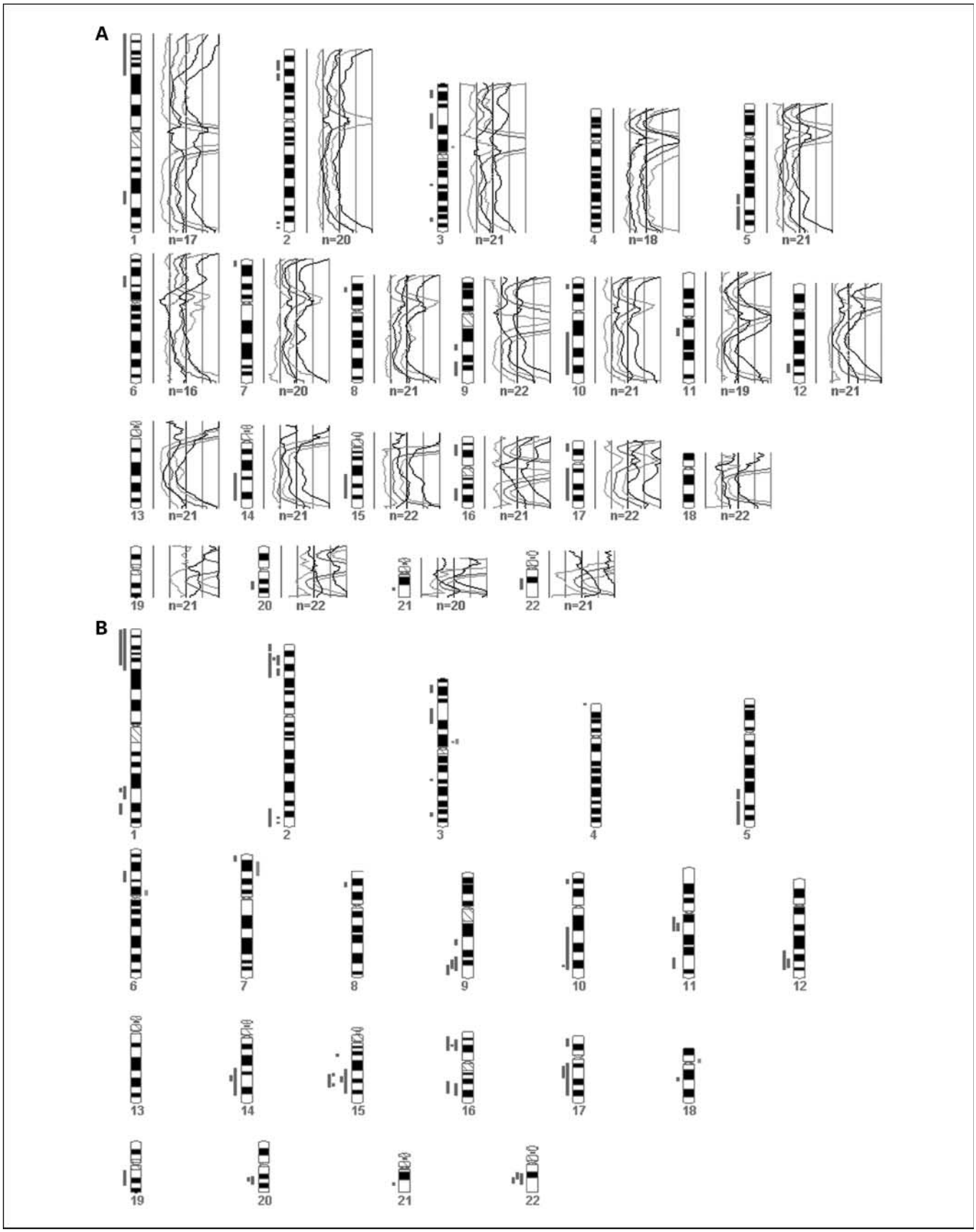

Fig. 5. Chromosomal imbalanced aberrations as detected by CGH in a representative malignant TSGCT (*A,* case no. 6) and the summarizing illustration (*B*) of DNA gains and losses in six malignant TSGCTs tested. Bars, one tumor, with gains on the right and losses on the left of the ideogram of each chromosome.

TP53 genes per se, whereas functionally disabled P53 protein is accumulated because of alterations in other proteins modulating its turnover and activity. Despite the complexity of regulatory networks, this process is best understood with regard to the deregulation of the upstream effectors in the P53 tumor suppressor pathway, such as inhibition of MDM2 and/or $P14^{ARF}$ activation (18, 31). The latter two events can consequently confer more aggressive behavior in transformed cells, as exemplified in both animal models and human cancer specimens (18, 31).

Chromosomal abnormalities point toward genes implicated in malignant transformation and disease progression (15, 16, 32). In this series, no imbalances were detected in any benign D-TSGCT by CGH, which, in keeping with the previous report (6), was most likely overshadowed by the diluted artifact of abundant inflammatory cells. In contrast, the sarcomatous areas of all six malignant lesions displayed varying numbers of chromosomal aberrations, predominantly in the form of chromosomal losses. The deletion at 15q, as detected in five cases, represented the most frequent non–random chromosomal alteration in malignant D-TSGCTs. Unlike hematologic malignancies, this aberration was only rarely documented by CGH in a few types of sarcomas, such as gastrointestinal intestinal tumors (33), endometrial stromal sarcomas (34), and osteosarcomas (35). Of special note, there were several P53-interacting genes located within the 19.3-Mb region of a common deletion at 15q22-24, such as *RPS27L* (15q22.2; ref. 36), *PIAS1* (15q22.3; ref. 37), *PML* (15q22; ref. 38), and *SIN3A* (15q24.2; ref. 39). Among these, *PML* is an established tumor suppressor gene critical in the formation of the PML nuclear body by recruiting P53 (38, 40, 41), whereas *RPS27L*, encoding a novel ribosomal protein, may represent another candidate (36). More intriguingly, sequences in the intron 1 region of both genes can be bound by P53 to mediate its proapoptotic and/or antiproliferative functions upon cellular stresses (36, 40, 41). In this context, we postulate a model wherein oncogenic signaling abnormality (e.g., *COL6A3-CSF1* gene fusion) may initially drive the development of benign D-TSGCT and elicit cellular responses mediated by wild-type P53. Nevertheless, sarcomatous transformation may arise once one or more P53-interacting tumor suppressor gene(s) within 15q22-24 is deleted, thereby compromising the tumor-suppressing function of P53.

In summary, we have, for the first time, provided evidence of *CSF1* involvement in malignant D-TSGCTs and described potential molecular markers to help differentiate malignant from benign lesions. As compared with benign lesions, alterations in cyclin A, P53, and chromosome arm 15q are present in the majority of malignant D-TSGCTs, representative of critical events in sarcomatous transformation. Cyclin A overexpression in malignant D-TSGCTs can be ascribed to high levels of *cyclin A* transcripts. Instead of intragenic mutations in hotspot exons, P53 overexpression is likely to be caused by alternative mechanisms leading to the stabilization of wild-type P53 protein. Furthermore, frequent deletions at 15q22-24 suggest the presence of candidate tumor suppressor gene(s) in this region, functional abrogation of which may render malignant phenotypes of this rare entity. To test this hypothetical model of malignant progression, additional studies are required with a large series of benign and malignant D-TSGCTs to further delineate the deleted tumor suppressor gene(s) of pathogenetic relevance within 15q22-24.

Disclosure of Potential Conflicts of Interest

No potential conflicts of interest were disclosed.

Acknowledgments

The authors are very grateful to Drs. Andrew G. Huvos and Cristina R. Antonescu at the Department of Pathology, Memorial Sloan-Kettering Cancer Center, and Dr. Jason L. Hornick at the Department of Pathology, Brigham and Women's Hospital, for their critical histological reviews of diagnoses.

References

1. Somerhausen NS, Fletcher CD. Diffuse-type giant cell tumor: clinicopathologic and immunohistochemical analysis of 50 cases with extraarticular disease. Am J Surg Pathol 2000;24:479–92.
2. Somerhausen NS, Dal Cin P. Diffuse-type tenosynovial giant cell tumor. In: Fletcher CDM, Unni KK, Mertens F, editors. WHO classification of tumors—pathology and genetics, tumors of soft tissue and bone. Lyon: IARC Press; 2002. p. 112–4.
3. Abdul-Karim FW, el-Naggar AK, Joyce MJ, Makley JT, Carter JR. Diffuse and localized tenosynovial giant cell tumor and pigmented villonodular synovitis: a clinicopathologic and flow cytometric DNA analysis. Hum Pathol 1992;23:729–35.
4. Sciot R, Rosai J, Dal Cin P, et al. Analysis of 35 cases of localized and diffuse tenosynovial giant cell tumor: a report from the Chromosomes and Morphology (CHAMP) study group. Mod Pathol 1999;12:576–9.
5. Layfield LJ, Meloni-Ehrig A, Liu K, Shepard R, Harrelson JM. Malignant giant cell tumor of synovium (malignant pigmented villonodular synovitis). Arch Pathol Lab Med 2000;124:1636–41.
6. Brandal P, Bjerkehagen B, Heim S. Molecular cytogenetic characterization of tenosynovial giant cell tumors. Neoplasia 2004;6:578–83.
7. Li CF WJ, Huang WW, Hou CC, et al. Malignant diffuse-type tenosynovial giant cell tumors: a series of 7 cases in comparison with 24 benign lesions and review of the literature. Am J Surg Pathol 2008;32:587–99.
8. Enzinger FM, Weiss S. Benign tumors and tumor-like lesions of synovial tissue. Soft tissue tumors. 3rd ed. St. Louis (MO). 1995. p. 735–55.
9. Bertoni F, Unni KK, Beabout JW, Sim FH. Malignant giant cell tumor of the tendon sheaths and joints (malignant pigmented villonodular synovitis). Am J Surg Pathol 1997;21:153–63.
10. Bhadra AK, Pollock R, Tirabosco RP, et al. Primary tumours of the synovium: a report of four cases of malignant tumour. J Bone Joint Surg Br 2007;89:1504–8.
11. West RB, Rubin BP, Miller MA, et al. A landscape effect in tenosynovial giant-cell tumor from activation of CSF1 expression by a translocation in a minority of tumor cells. Proc Natl Acad Sci U S A 2006;103:690–5.
12. Borden EC, Baker LH, Bell RS, et al. Soft tissue sarcomas of adults: state of the translational science. Clin Cancer Res 2003;9:1941–56.
13. Huang HY, Illei PB, Zhao Z, et al. Ewing sarcomas with p53 mutation or p16/p14ARF homozygous deletion: a highly lethal subset associated with poor chemoresponse. J Clin Oncol 2005;23:548–58.
14. Ozaki T, Paulussen M, Poremba C, et al. Genetic imbalances revealed by comparative genomic hybridization in Ewing tumors. Genes Chromosomes Cancer 2001;32:164–71.
15. Kallioniemi A, Kallioniemi OP, Sudar D, et al. Comparative genomic hybridization for molecular cytogenetic analysis of solid tumors. Science 1992;258:818–21.
16. Kallioniemi OP, Kallioniemi A, Piper J, et al. Optimizing comparative genomic hybridization for analysis of DNA sequence copy number changes in solid tumors. Genes Chromosomes Cancer 1994;10:231–43.
17. Cupp JS, Miller MA, Montgomery KD, et al. Translocation and expression of CSF1 in pigmented villonodular synovitis, tenosynovial giant cell tumor, rheumatoid arthritis and other reactive synovitides. Am J Surg Pathol 2007;31:970–6.
18. Wang YC, Lin RK, Tan YH, Chen JT, Chen CY, Wang YC. Wild-type p53 overexpression and its correlation with MDM2 and p14ARF alterations: an alternative pathway to non-small-cell lung cancer. J Clin Oncol 2005;23:154–64.
19. Radonic A, Thulke S, Mackay IM, Landt O, Siegert W, Nitsche A. Guideline to reference gene selection for quantitative real-time PCR. Biochem Biophys Res Commun 2004;313:856–62.
20. Livak KJ, Schmittgen TD. Analysis of relative gene expression data using real-time quantitative PCR and the 2(-ΔΔC(T)) method. Methods 2001;25:402–8.

21. Lehmann U, Kreipe H. Real-time PCR analysis of DNA and RNA extracted from formalin-fixed and paraffin-embedded biopsies. Methods 2001;25:409–18.

22. Kirchhoff M, Gerdes T, Rose H, Maahr J, Ottesen AM, Lundsteen C. Detection of chromosomal gains and losses in comparative genomic hybridization analysis based on standard reference intervals. Cytometry 1998;31:163–73.

23. Moller E, Mandahl N, Mertens F, Panagopoulos I. Molecular identification of COL6A3-1 fusion transcripts in tenosynovial giant cell tumors. Genes Chromosomes Cancer 2008;47:21–5.

24. Yam CH, Fung TK, Poon RY. Cyclin A in cell cycle control and cancer. Cell Mol Life Sci 2002;59:1317–26.

25. Huuhtanen RL, Blomqvist CP, Bohling TO, et al. Expression of cyclin A in soft tissue sarcomas correlates with tumor aggressiveness. Cancer Res 1999;59:2885–90.

26. Xie Y, Skytting B, Nilsson G, et al. The SYT-SSX1 fusion type of synovial sarcoma is associated with increased expression of cyclin A and D1. A link between t(X;18)(p11.2; q11.2) and the cell cycle machinery. Oncogene 2002;21:5791–6.

27. Ashcroft M, Vousden KH. Regulation of p53 stability. Oncogene 1999;18:7637–43.

28. Sionov RV, Haupt Y. The cellular response to p53: the decision between life and death. Oncogene 1999;18:6145–57.

29. Das P, Kotilingam D, Korchin B, et al. High prevalence of p53 exon 4 mutations in soft tissue sarcoma. Cancer 2007;109:2323–33.

30. Petitjean A, Mathe E, Kato S, et al. Impact of mutant p53 functional properties on TP53 mutation patterns and tumor phenotype: lessons from recent developments in the IARC TP53 database. Hum Mutat 2007;28:622–9.

31. Sherr CJ. The INK4a/ARF network in tumour suppression. Nat Rev Mol Cell Biol 2001;2:731–7.

32. Jefford CE, Irminger-Finger I. Mechanisms of chromosome instability in cancers. Crit Rev Oncol Hematol 2006;59:1–14.

33. Wozniak A, Sciot R, Guillou L, et al. Array CGH analysis in primary gastrointestinal stromal tumors: cytogenetic profile correlates with anatomic site and tumor aggressiveness, irrespective of mutational status. Genes Chromosomes Cancer 2007;46:261–76.

34. Halbwedl I, Ullmann R, Kremser ML, et al. Chromosomal alterations in low-grade endometrial stromal sarcoma and undifferentiated endometrial sarcoma as detected by comparative genomic hybridization. Gynecol Oncol 2005;97:582–7.

35. dos Santos Aguiar S, de Jesus Girotto Zambaldi L, dos Santos AM, Pinto W, Jr., Brandalise SR. Comparative genomic hybridization analysis of abnormalities in chromosome 21 in childhood osteosarcoma. Cancer Genet Cytogenet 2007;175:35–40.

36. He H, Sun Y. Ribosomal protein S27L is a direct p53 target that regulates apoptosis. Oncogene 2007;26:2707–16.

37. Schmidt D, Muller S. Members of the PIAS family act as SUMO ligases for c-Jun and p53 and repress p53 activity. Proc Natl Acad Sci U S A 2002;99:2872–7.

38. Bernardi R, Pandolfi PP. Role of PML and the PML-nuclear body in the control of programmed cell death. Oncogene 2003;22:9048–57.

39. Murphy M, Ahn J, Walker KK, et al. Transcriptional repression by wild-type p53 utilizes histone deacetylases, mediated by interaction with mSin3a. Genes Dev 1999;13:2490–501.

40. Guo A, Salomoni P, Luo J, et al. The function of PML in p53-dependent apoptosis. Nat Cell Biol 2000;2:730–6.

41. de Stanchina E, Querido E, Narita M, et al. PML is a direct p53 target that modulates p53 effector functions. Mol Cell 2004;13:523–35.